

Workshop on Detectors for Synchrotron Research
October 30-31, 2000
Washington, DC

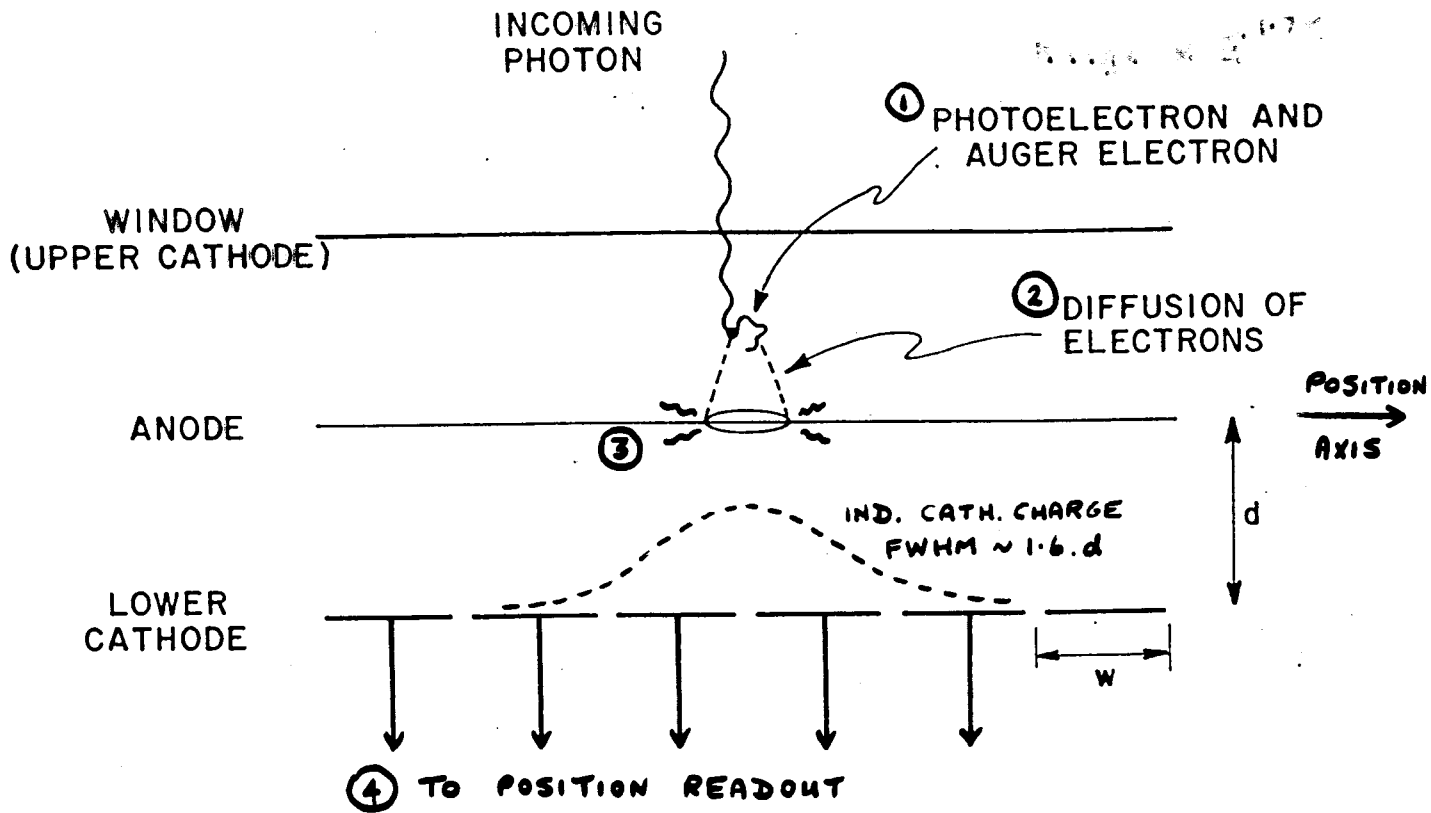
GAS DETECTORS

Graham Smith

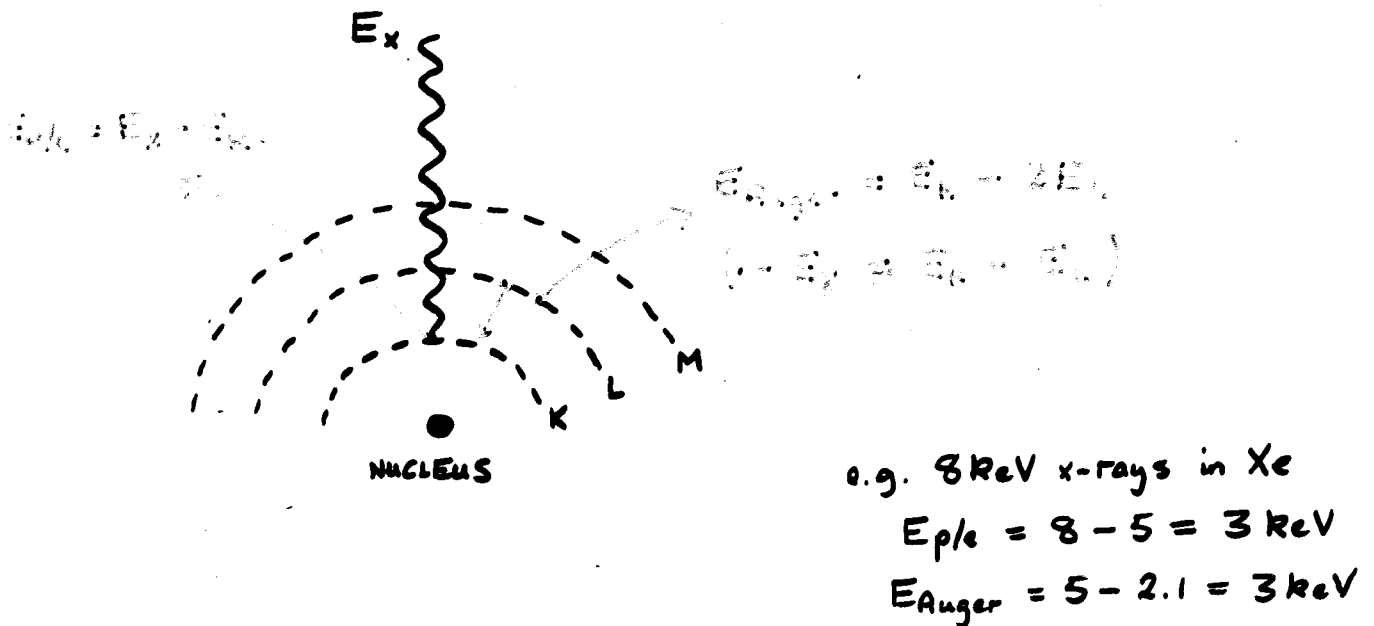
**Instrumentation Division
Brookhaven National Laboratory
Upton NY 11973**

- Position Encoding
Resolution
Linearity
- Photon counting $\approx 10^6$ Hz
- Recent Special Techniques
- Micropattern Detectors

⇒ Research Groups — only small nos. of detectors
Commercial Products — geared for profit

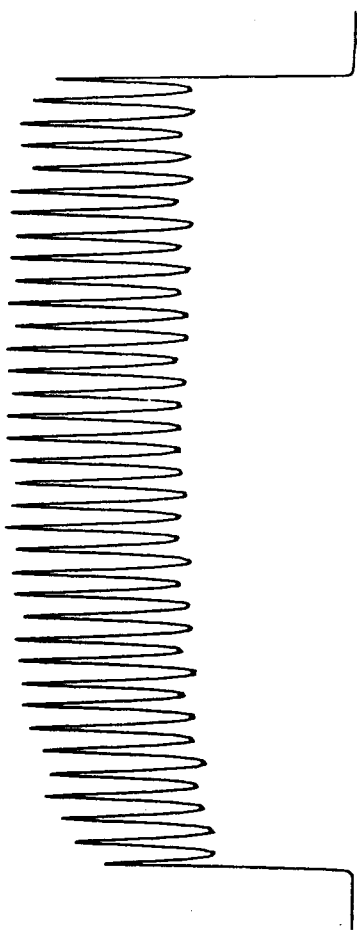
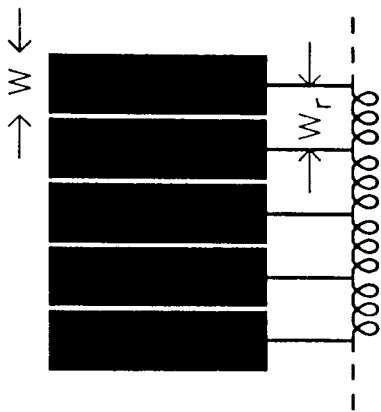


THE MOST IMPORTANT DISPERSIVE PHENOMENA WHICH AFFECT POSITION LINE WIDTH ARE ①, ②, ③ + ④. IN PRACTICAL MEASUREMENTS OF POSITION RESOLUTION, INSTRUMENTAL FACTORS SUCH AS FINITE X-RAY BEAM WIDTH ALSO NEED TO BE CONSIDERED

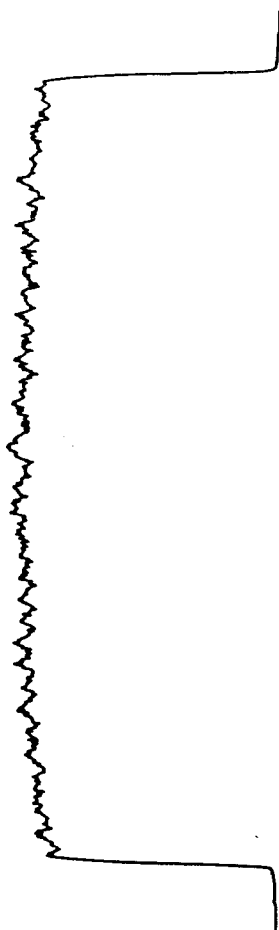
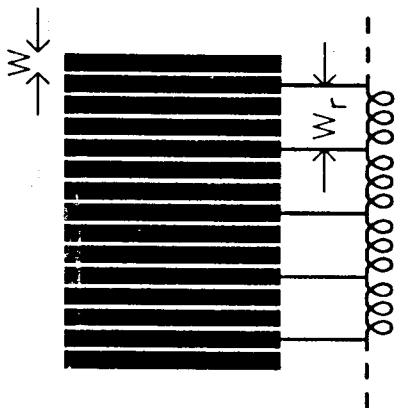


ELECTRODE TYPE

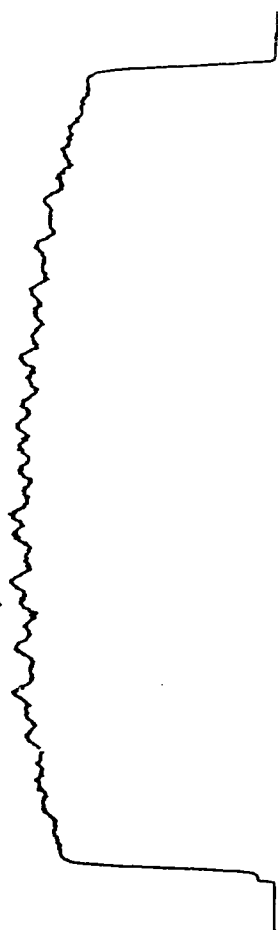
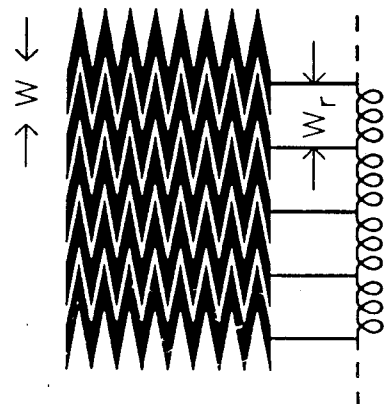
SIMPLE STRIP

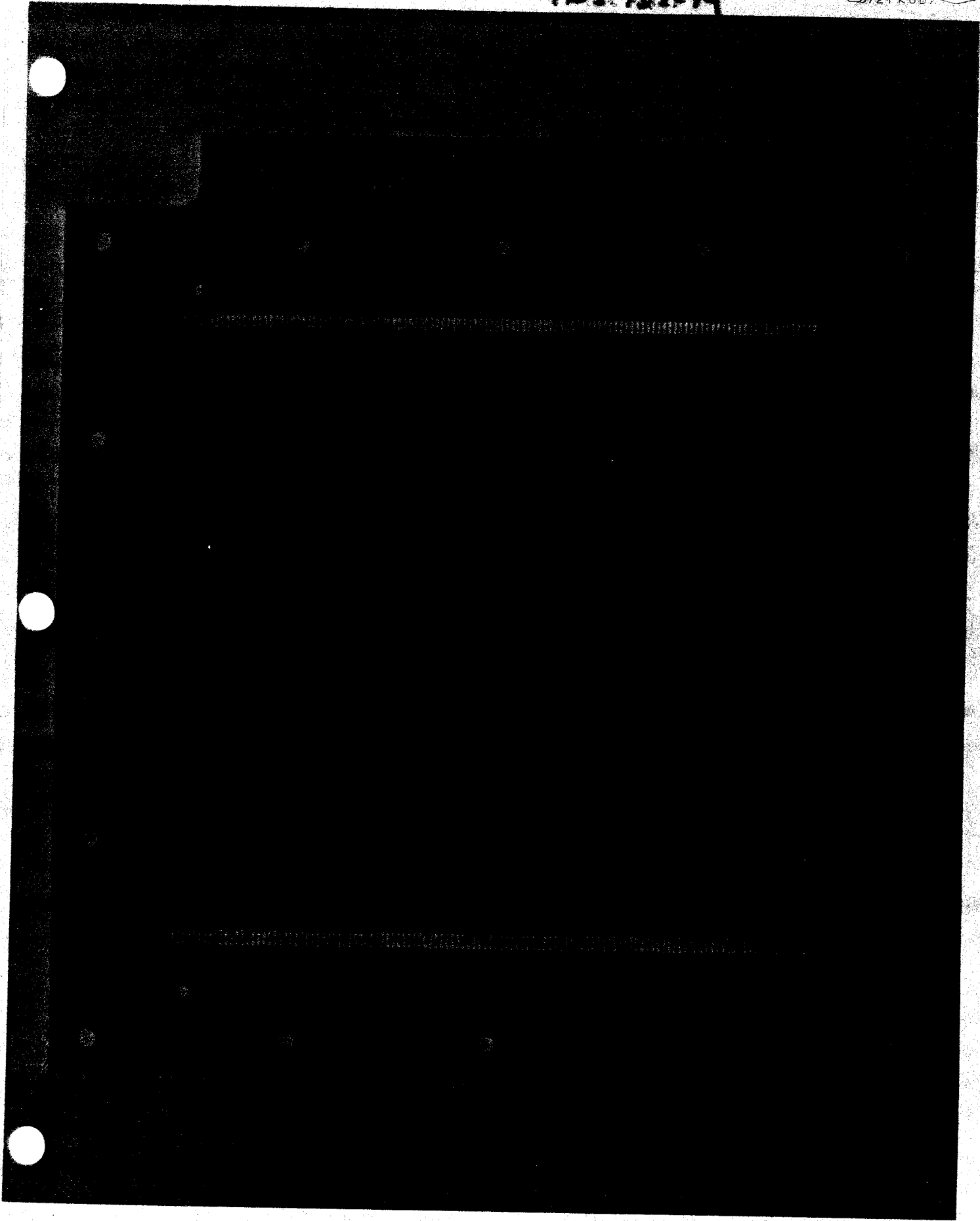


TWO INTERMEDIATE STRIP

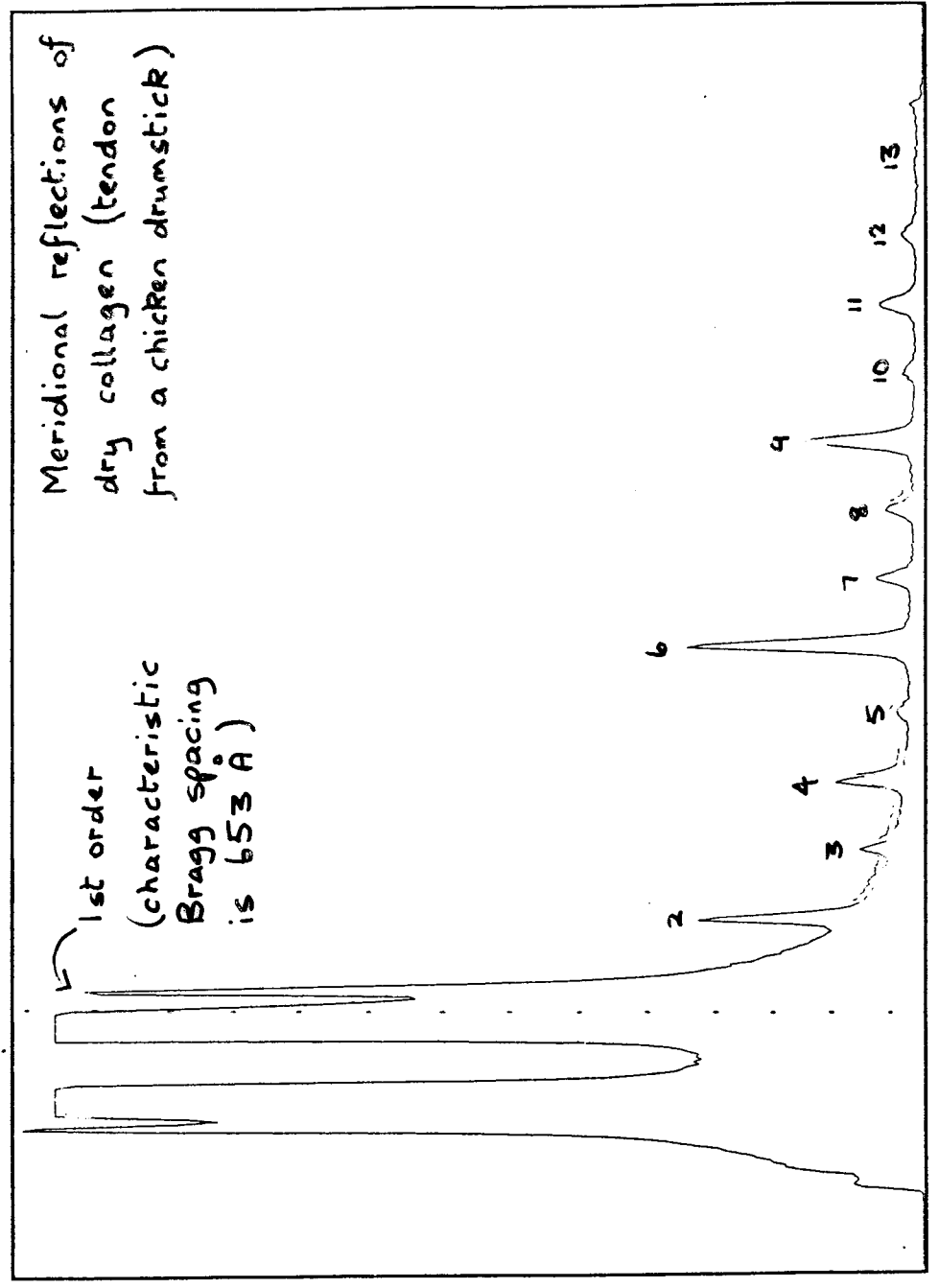
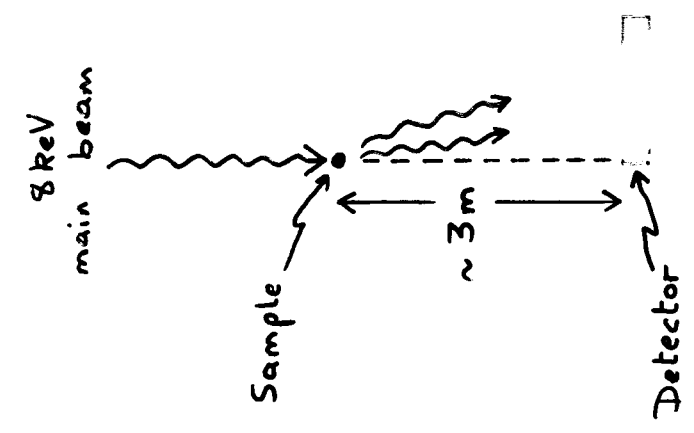


ZIG-ZAG



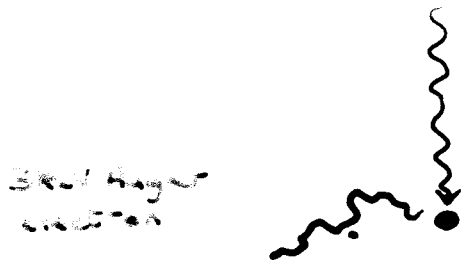


ONE DIMENSIONAL, DELAY LINE DETECTOR AT BEAM LINE X12B, NSLS

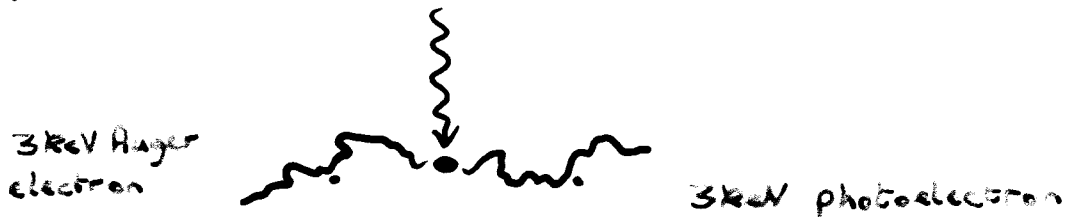


X-RAY ABSORPTION IN XENON (XE_L edge $\sim 5\text{keV}$
 XE_K edge = 34.6keV)

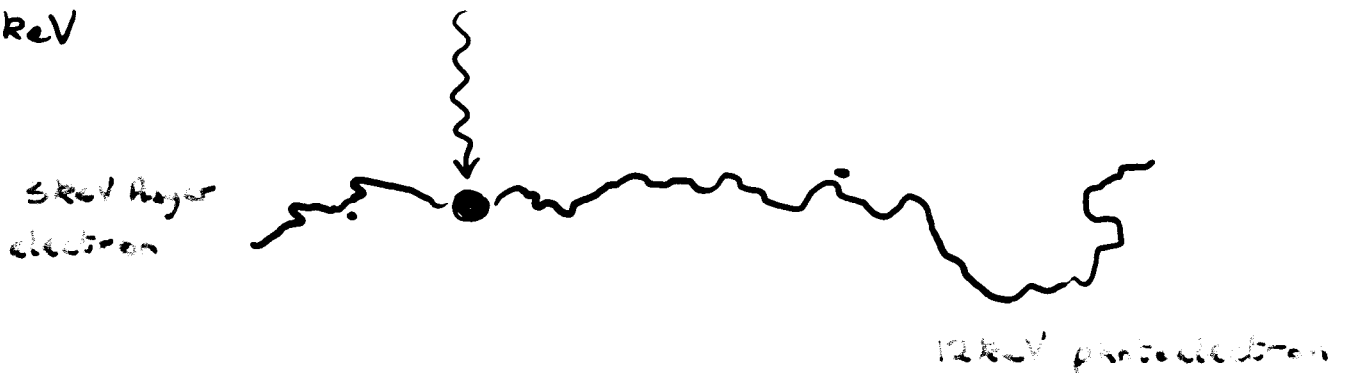
5 keV



8 keV



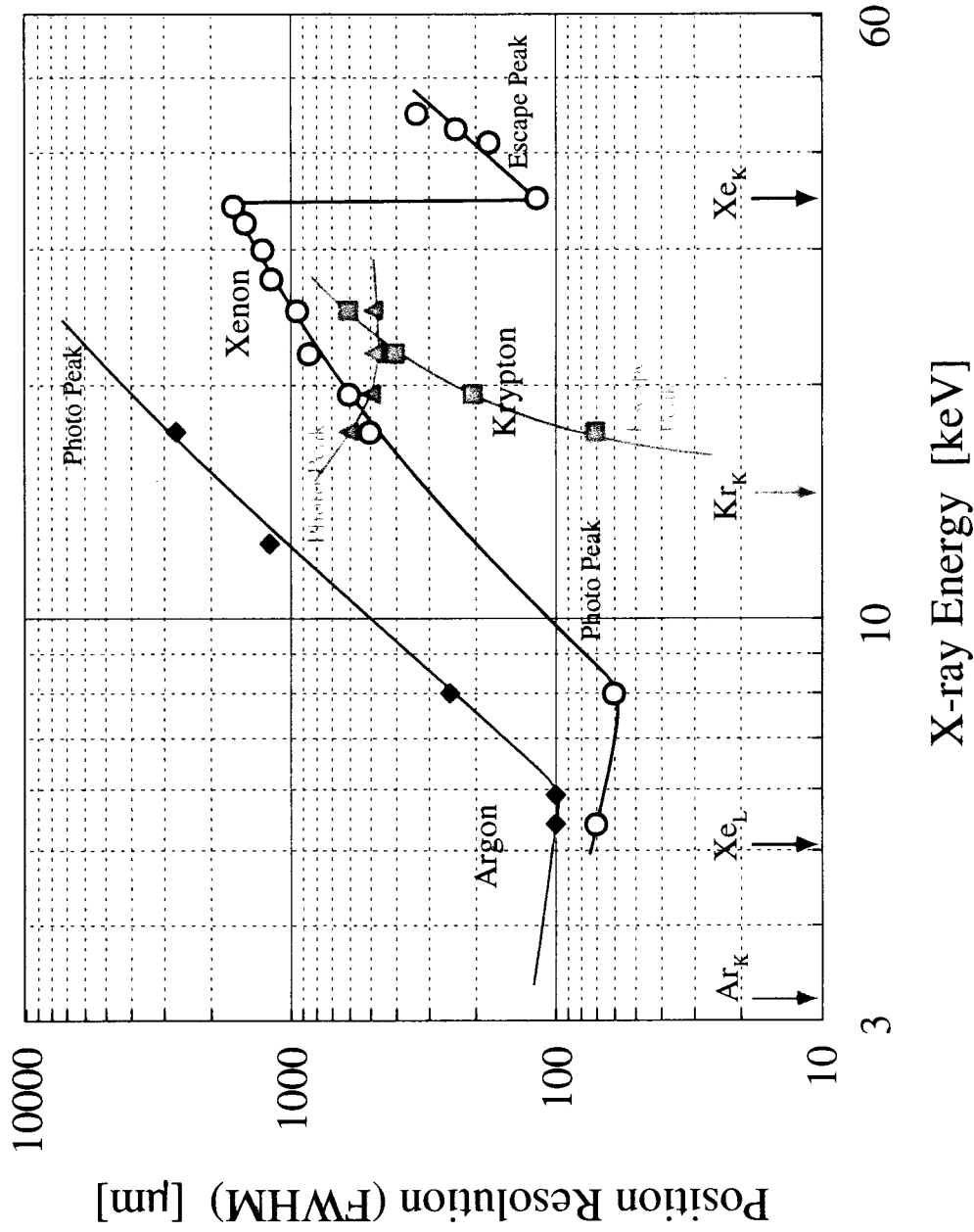
17 keV

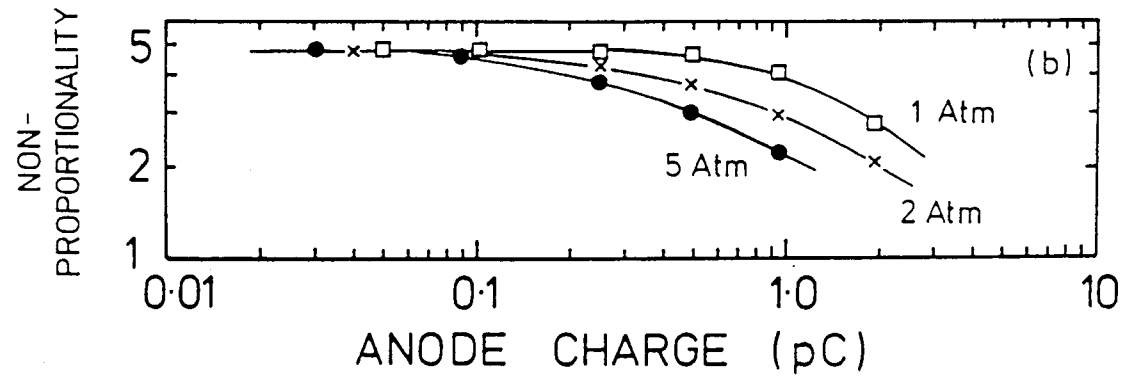
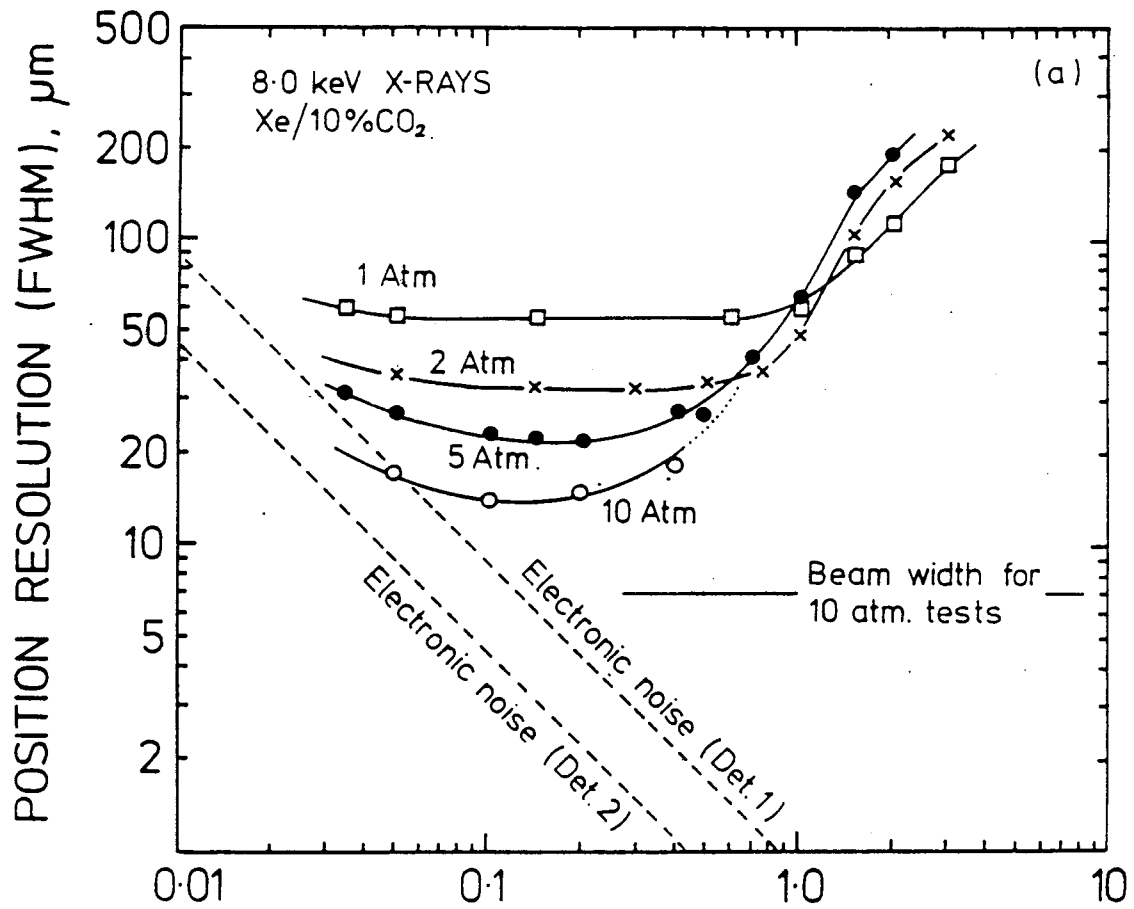


$$K_{\alpha} \times E_{\alpha}^{1/3}$$

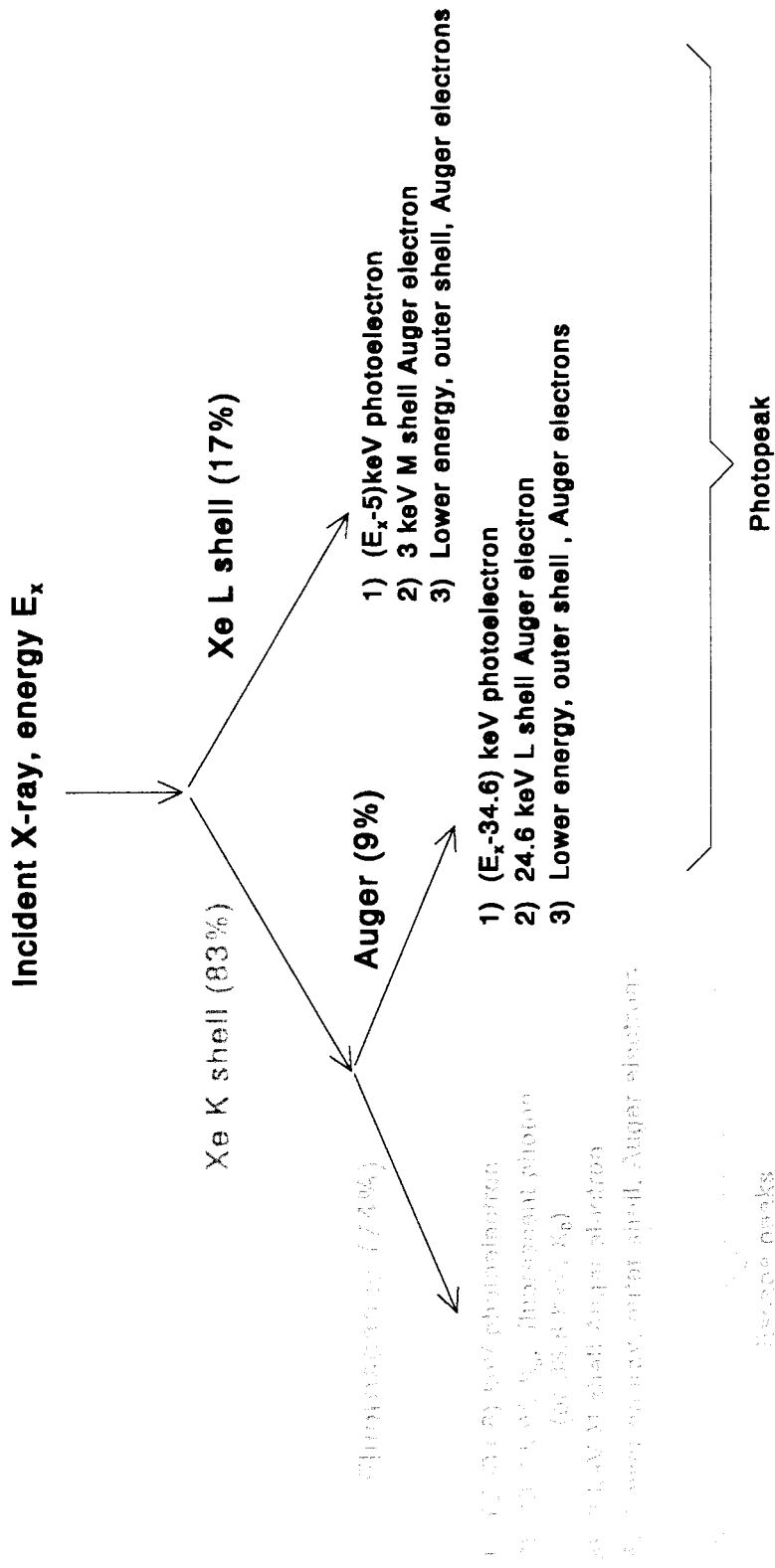
Exploring the Fundamental Limits in a MWPC

X-ray Position Resolution Limit of a Gas Detector Due to Electron Range (@ 1 atm.)

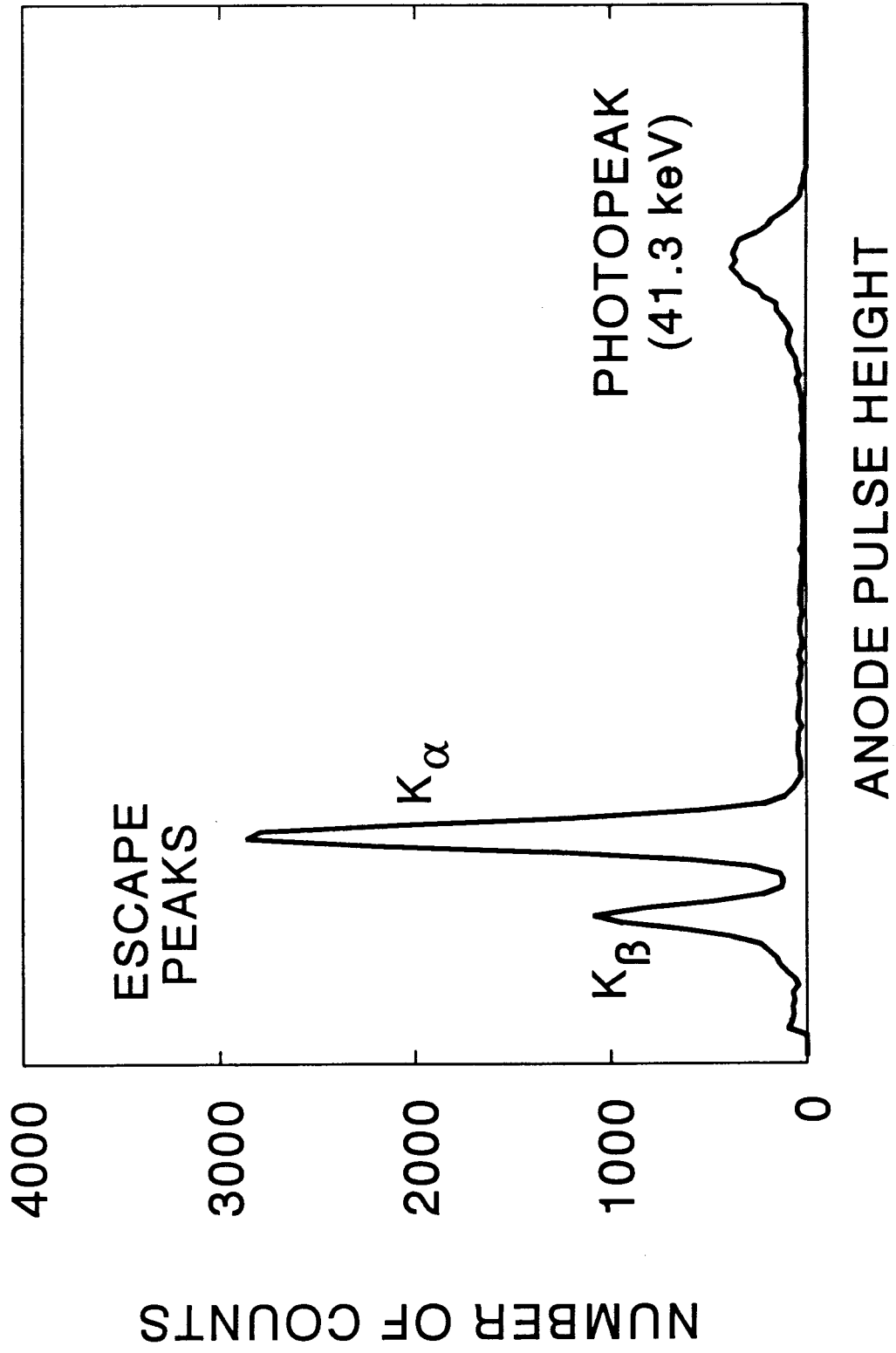




XENON ATOM DE-EXCITATION PATHS, $E_x > E_K$

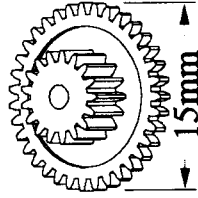


Energy Spectrum, 41.3 keV X-rays, 1 bar Xe/10%CO₂

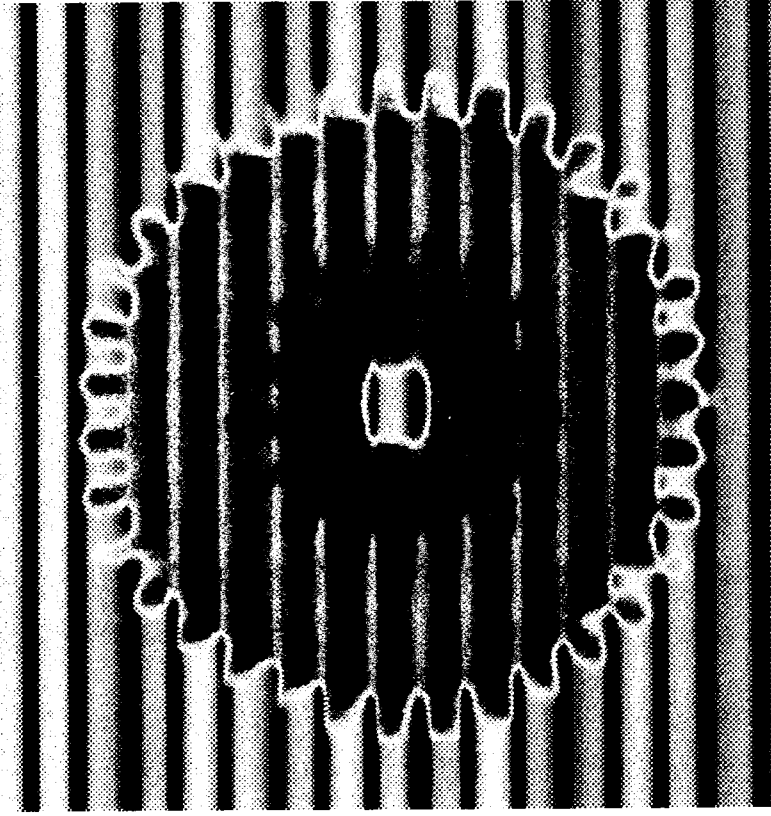
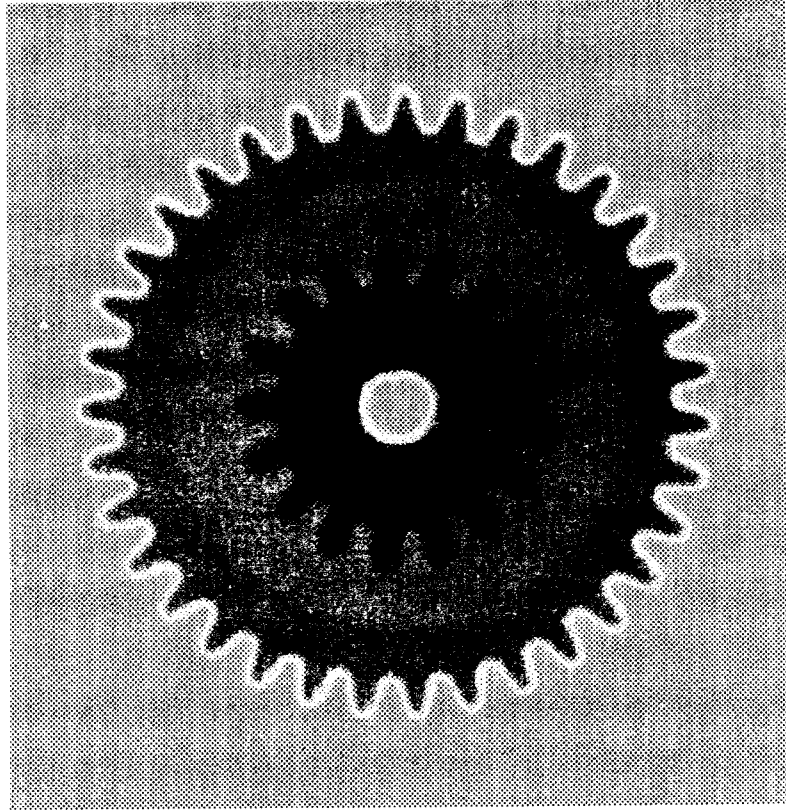


X-ray Images of a 15mm Diameter Plastic Gear Wheel

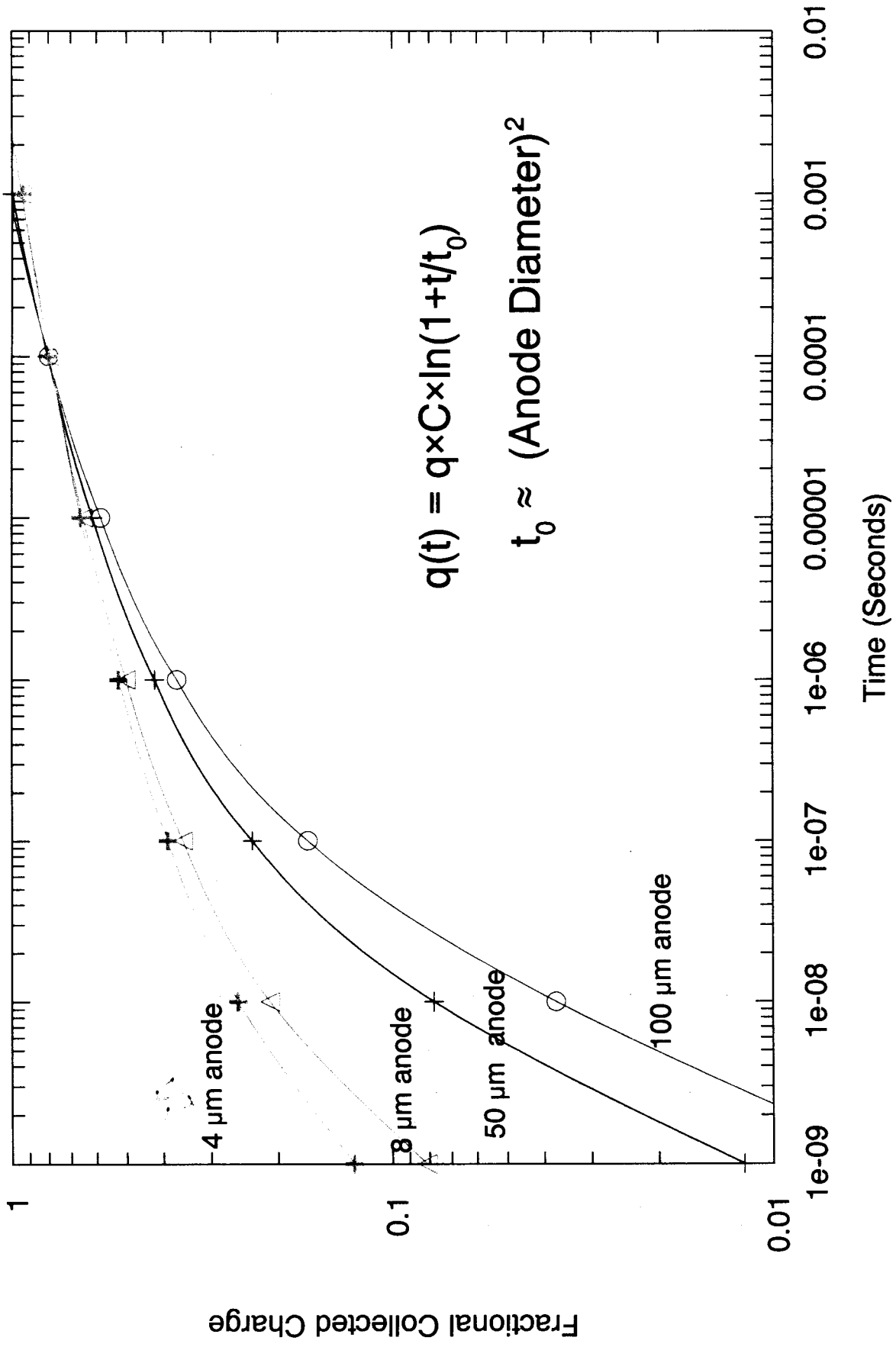
Anode wire pitch: 0.58mm
Cathode wire pitch: 0.58mm
(10x2 cm² 2D detector)



Anode wire pitch: 1.1mm
Cathode wire pitch: 0.48mm
(10x10 cm² 2D detector)

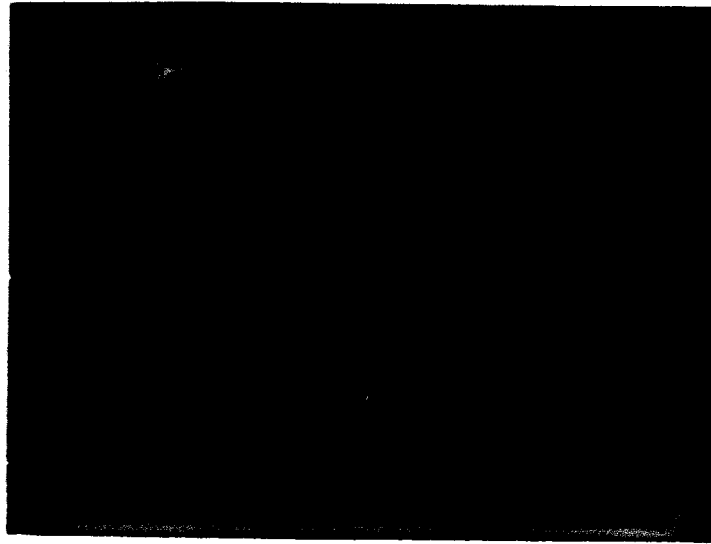


Time Development of Anode Charge



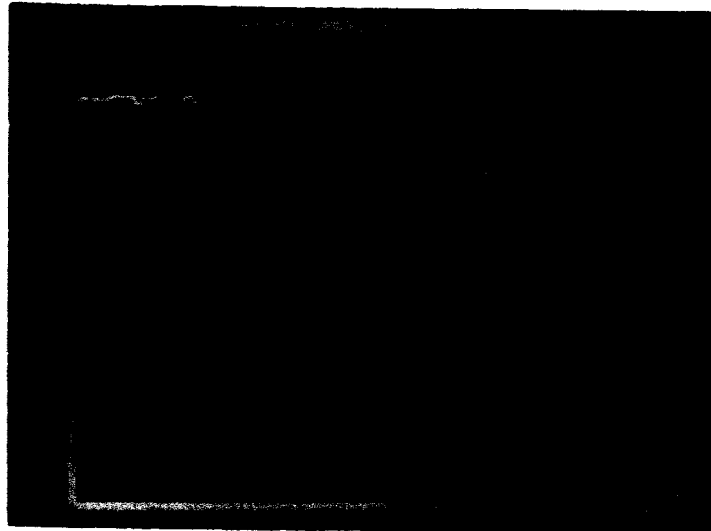
SINGLE CHANNEL SIGNAL WAVEFORMS

(a)



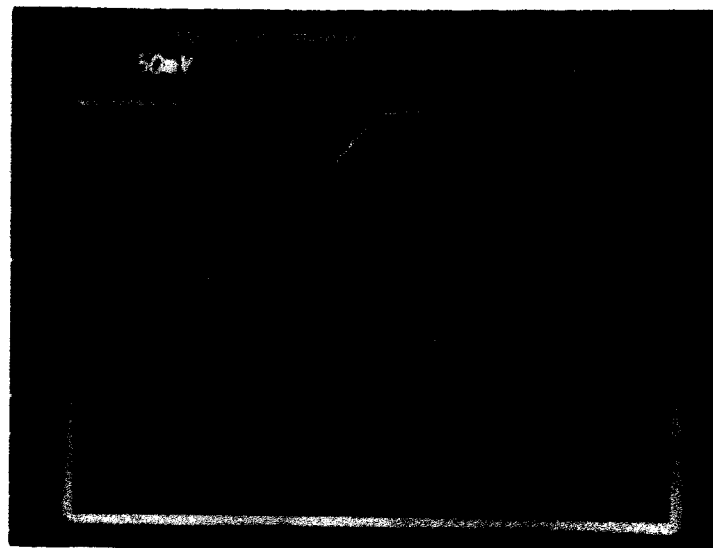
Preamp

(b)

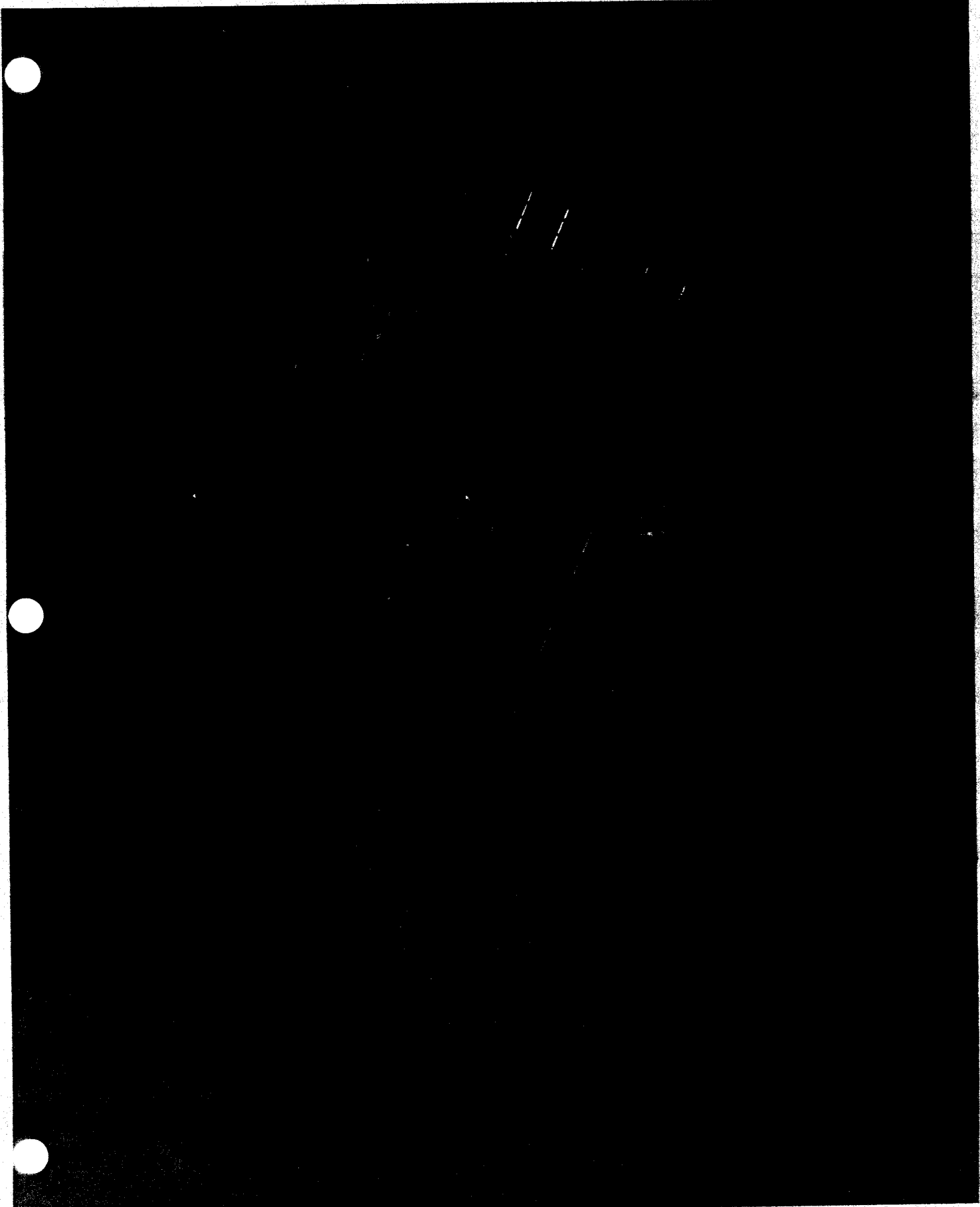


Preamp
+ pole zero
cancellation

(c)



Preamp
+ pole zero
+ ion tail
cancellation

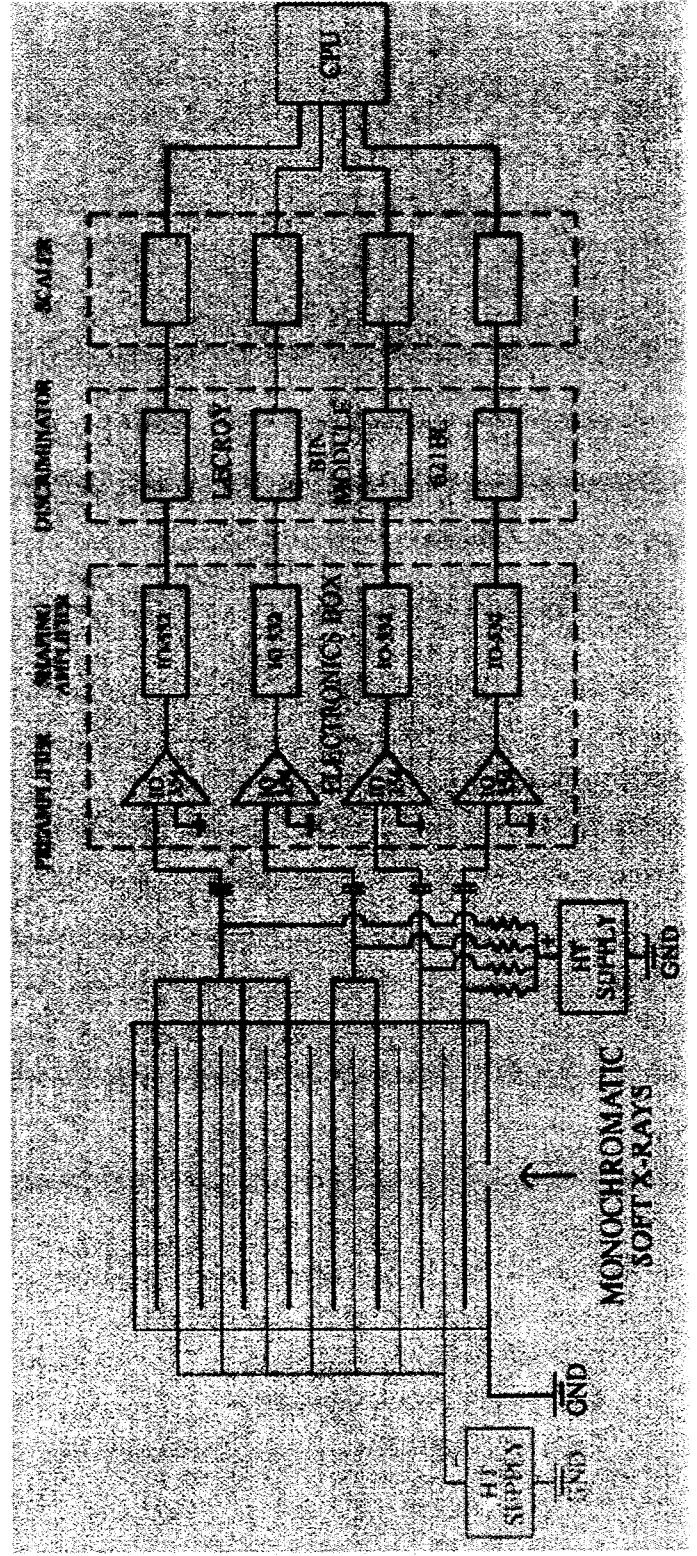
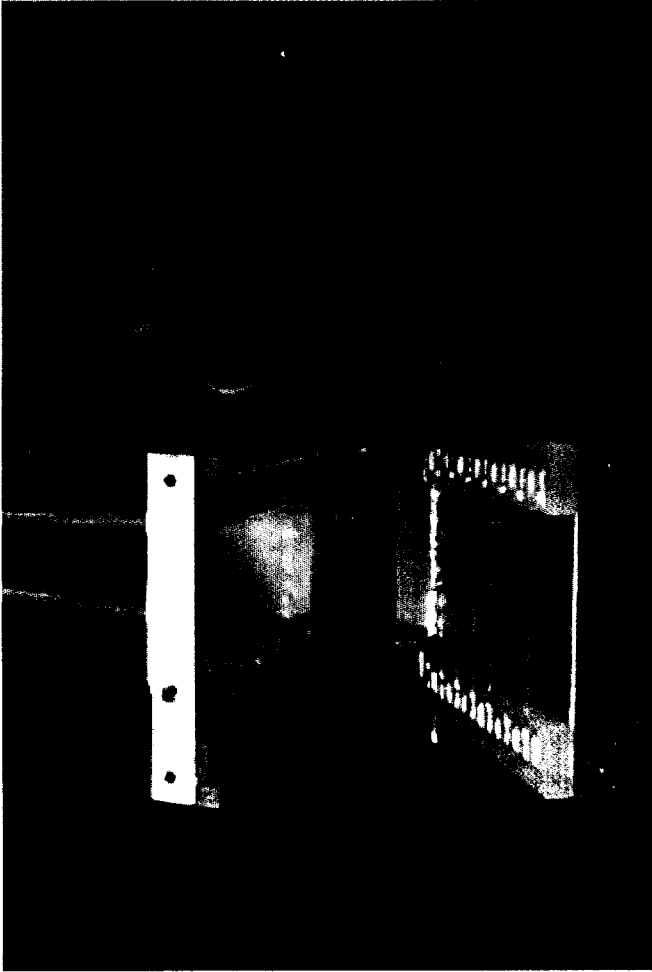


411 KODAK

411 KODAK

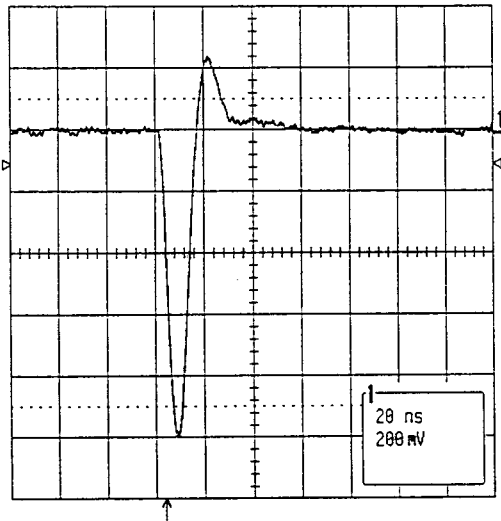
411 KODAK

Soft X-ray Proportional Chamber and Analysis Electronics

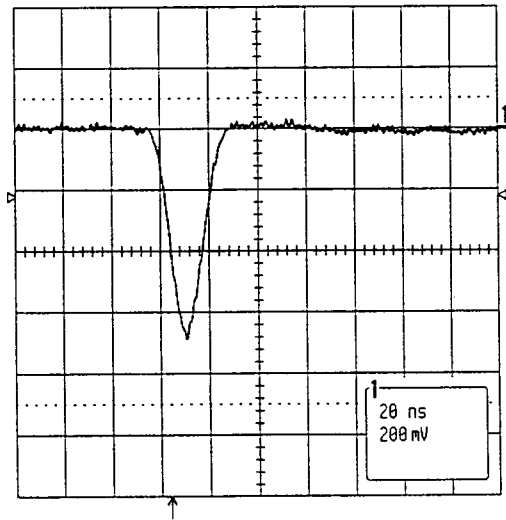


High Rate Gas Detector For Soft X-Ray Microscopy

Fast shaper output after pole-zero adjustment for positive-ion tail cancellation



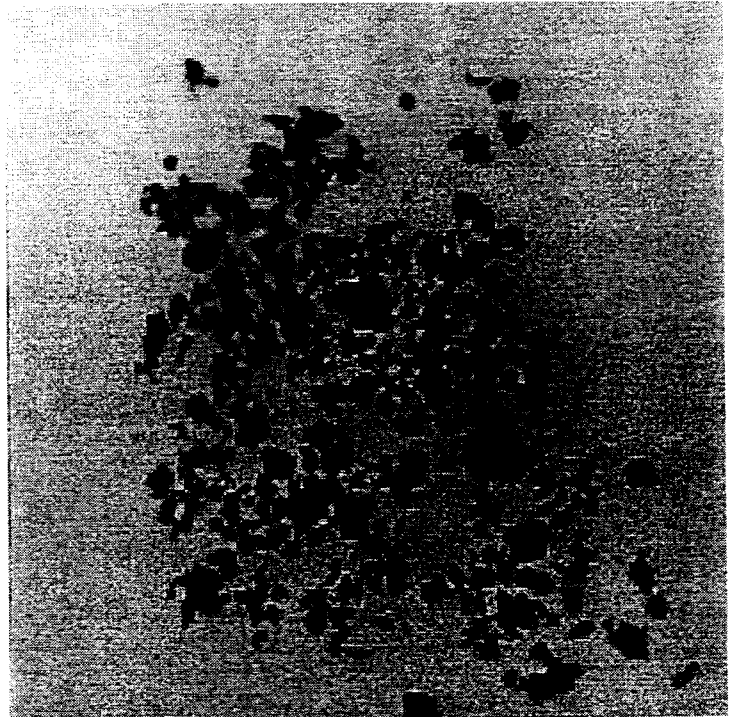
Step pulse response



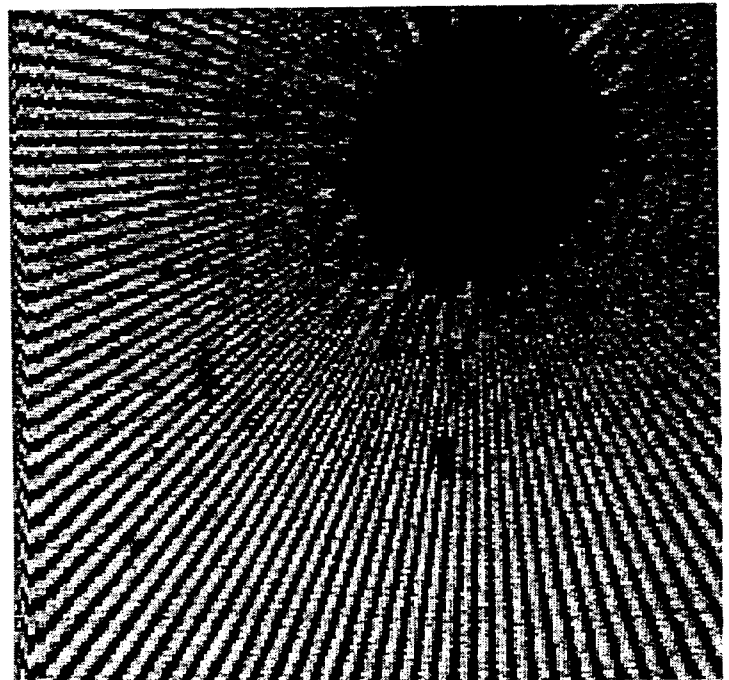
X-ray response

Image of test pattern with C_K X-rays. Lines on mask are nickel, width near center about 25nm

Images taken at beam-line X1A of NLSL using new detector

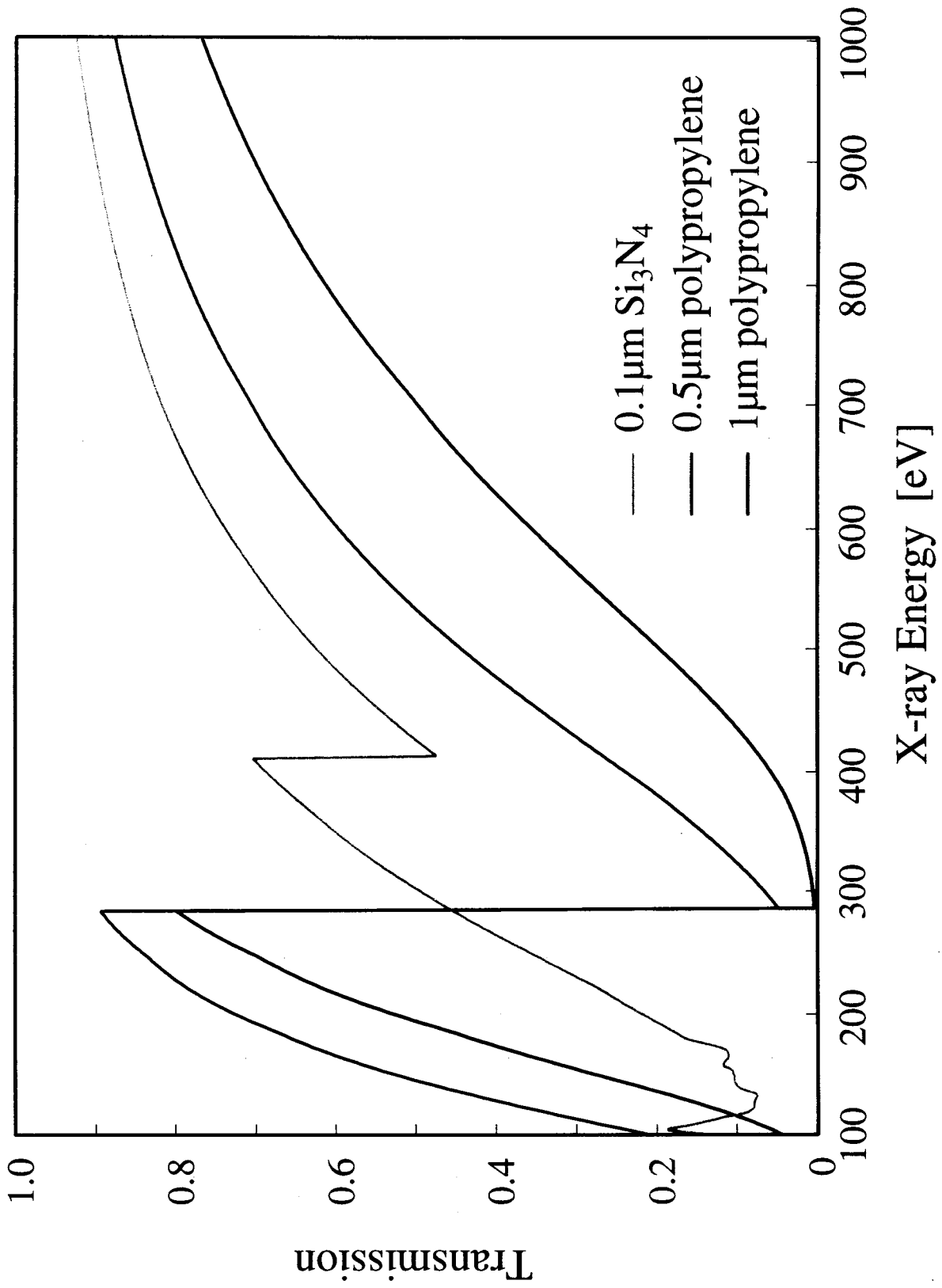


Flocculates in soil – study to reduce erosion in soil loam

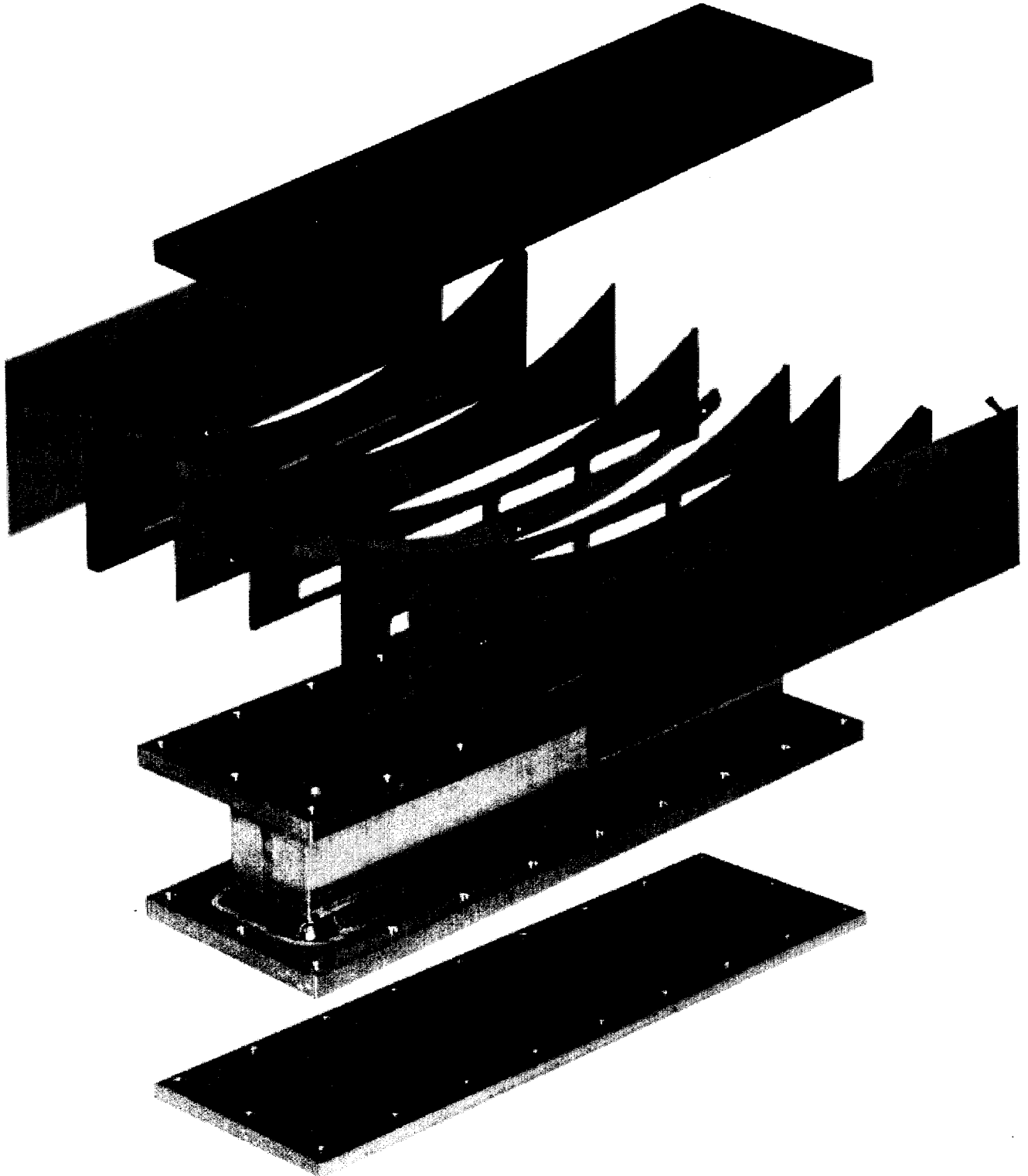


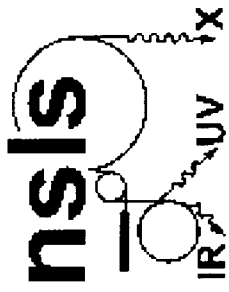
2 μ m Image of Testpattern

Soft X-ray Transmission of Detector Window Materials

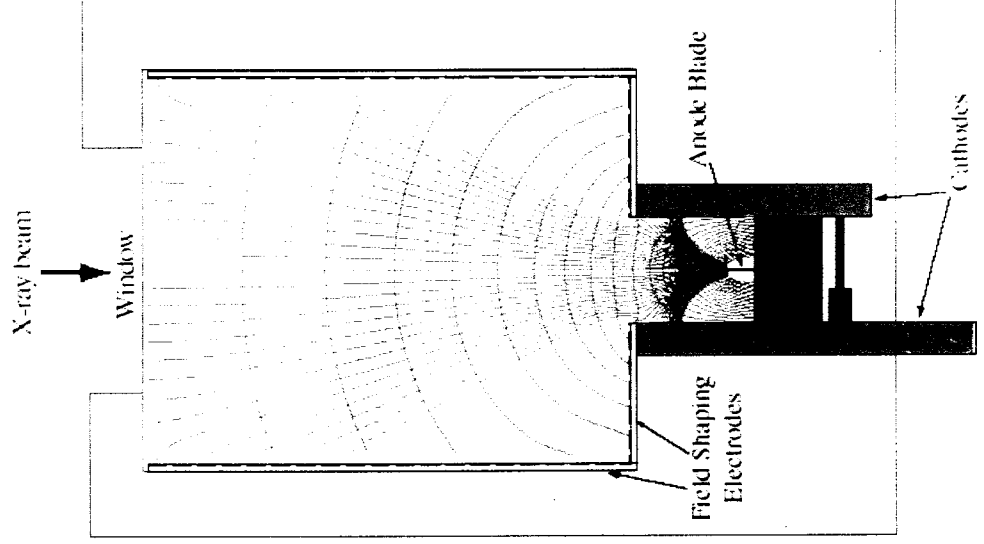


Component Parts of the Curved Blade Detector

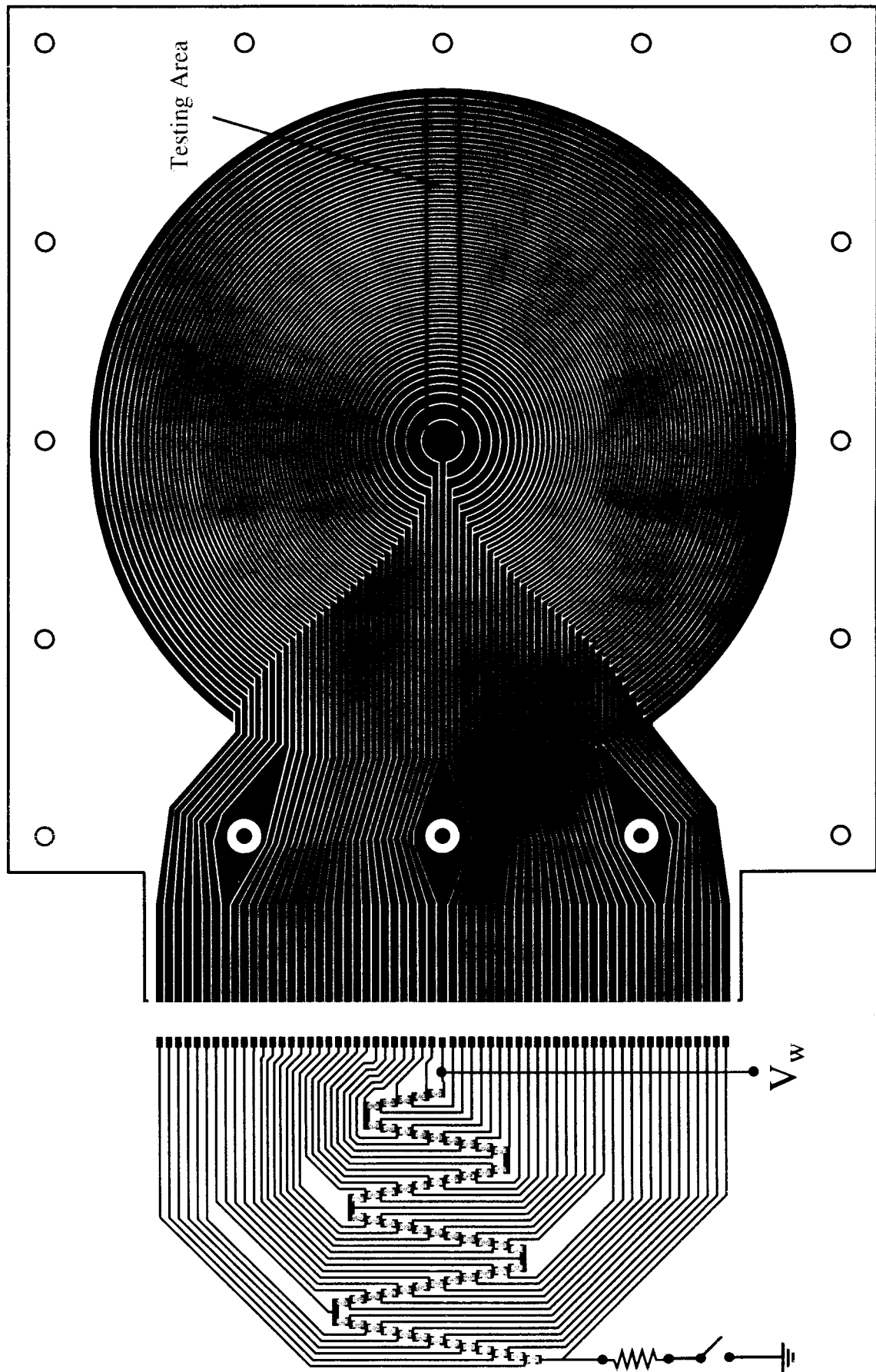




Cross-section of final electrode design

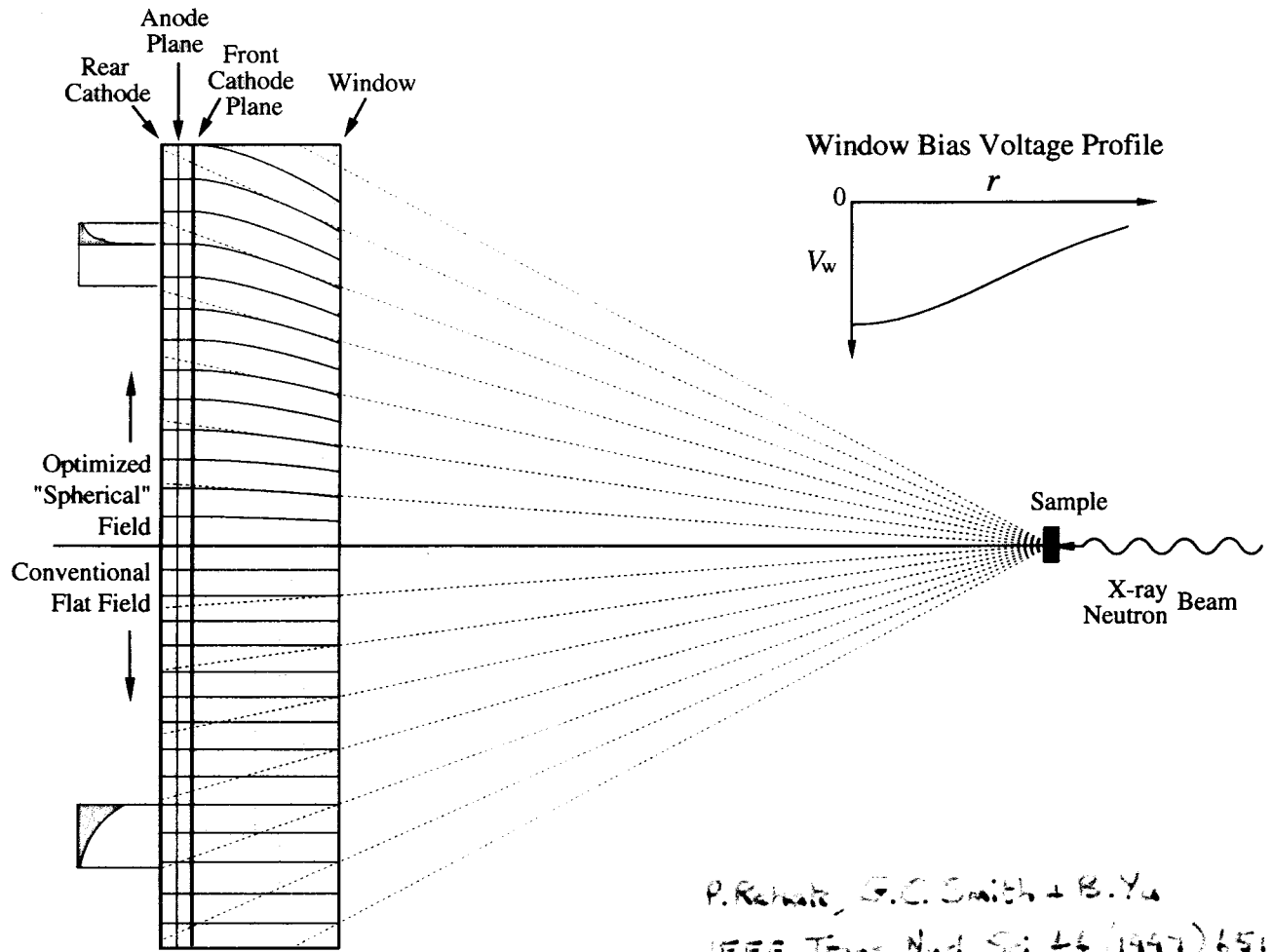


ELECTRODE PATTERN ON THE DETECTOR WINDOW

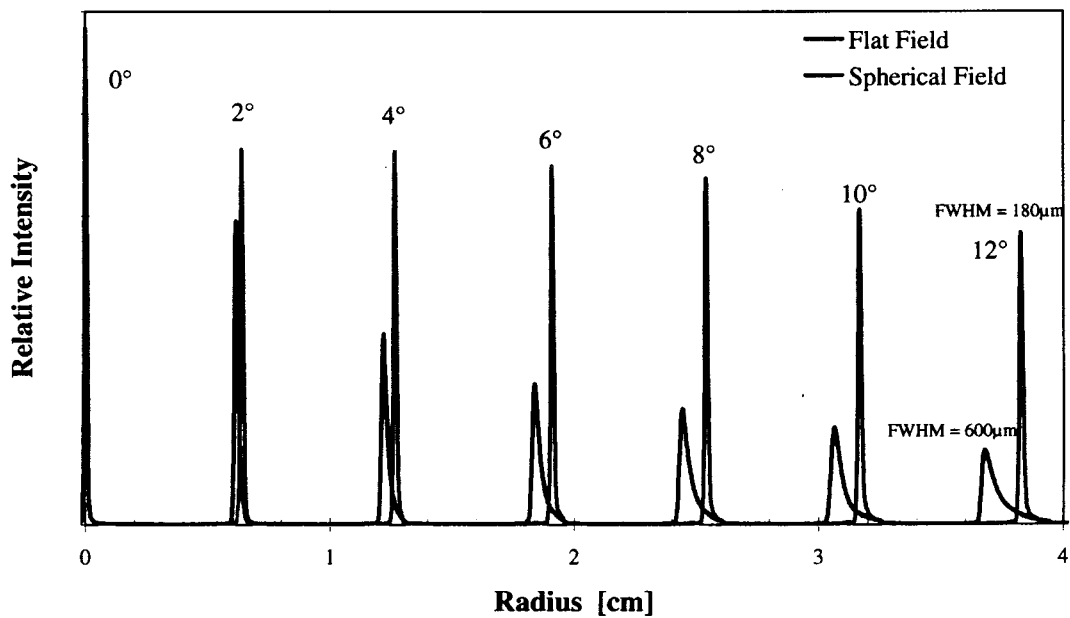


Window material is mylar sheet, with conducting annuli (black) from evaporated aluminum. The resistive divider at left applies potential which varies from 2.5kV on the central disc to 500V on the outer annulus.

PARALLAX REDUCTION TECHNIQUE



Detector Responses to Collimated Beam at Various Incident Angles
(5.4keV x-rays, Xenon+10%CO₂, 1.27cm Gas Depth, 18cm focal length)



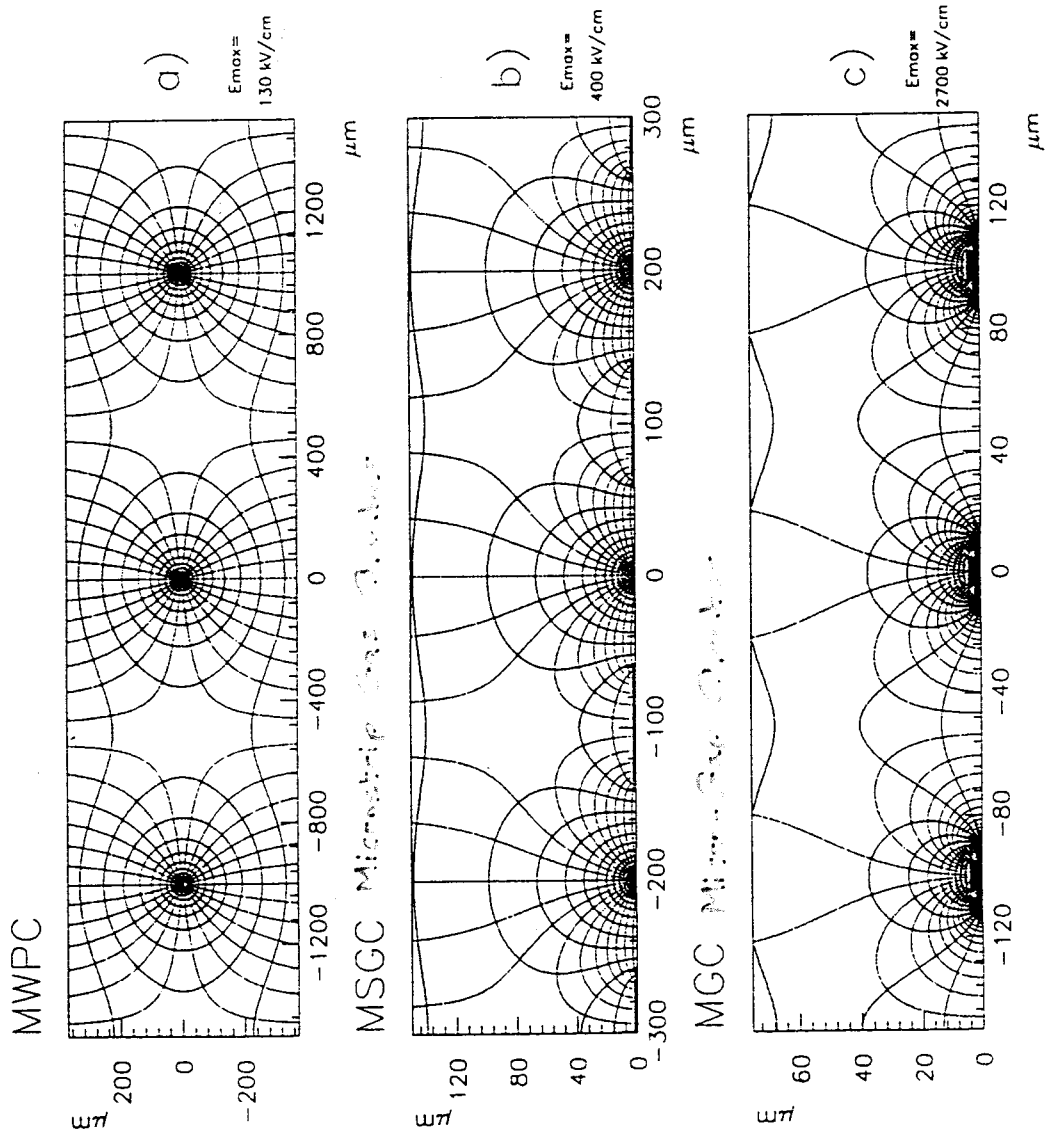


Fig. 3. Field and equipotential lines for a MWPC (a), for a MSGC (b) and for a MGC (c).

ing pitch).

An interesting property of Micromegas is that small variations of the amplification gap, due to mechanical defects, are compensated for by an inverse variation of the amplification factor. As shown in Fig. 2, for a given voltage applied in a thin parallel-plate chamber, the gain as a function

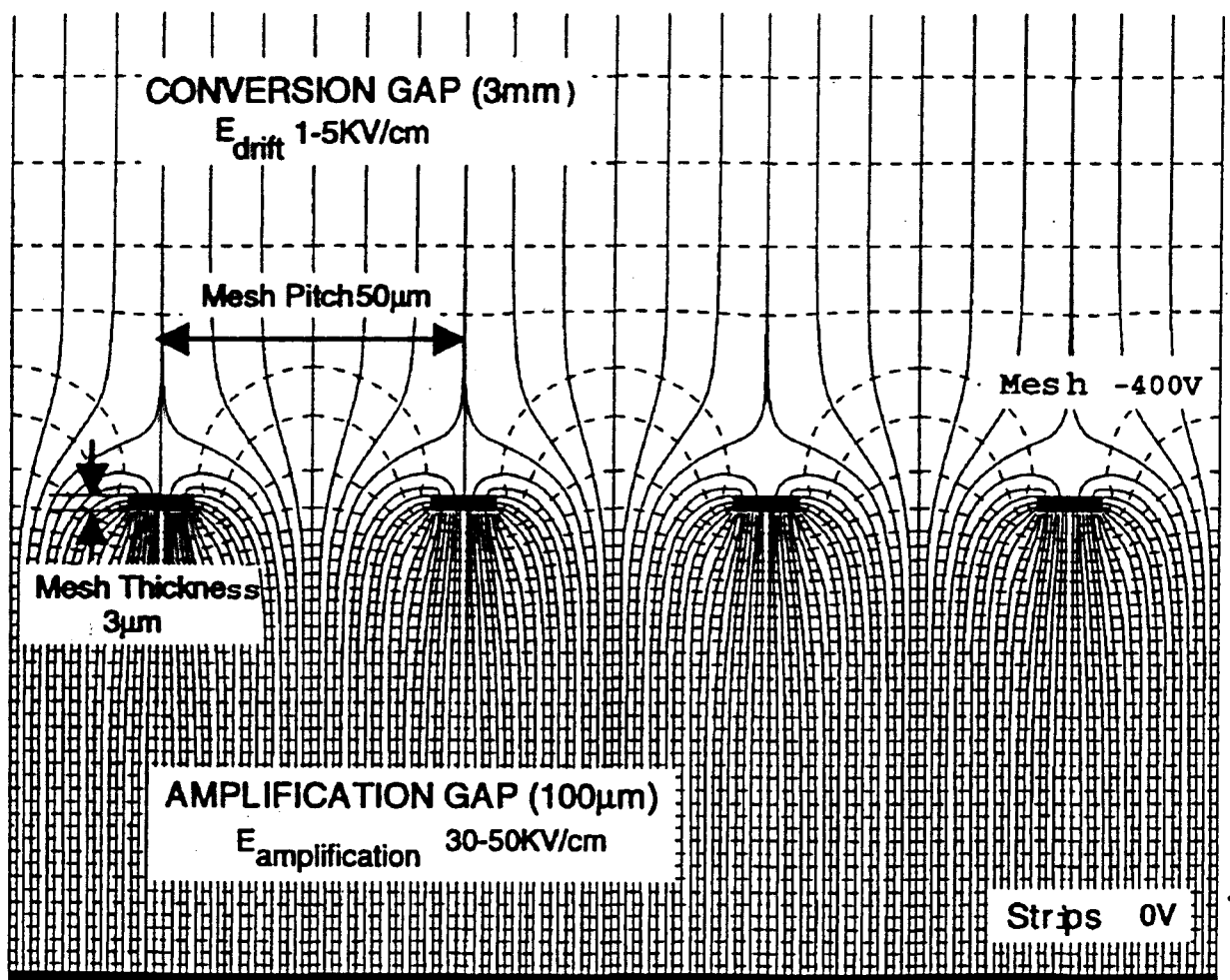


Fig. 1. Micromegas electric-field map.

YANNIS GIOMATARIS

NUCL. INSTR. & METH. A 419 (1998) 239-250

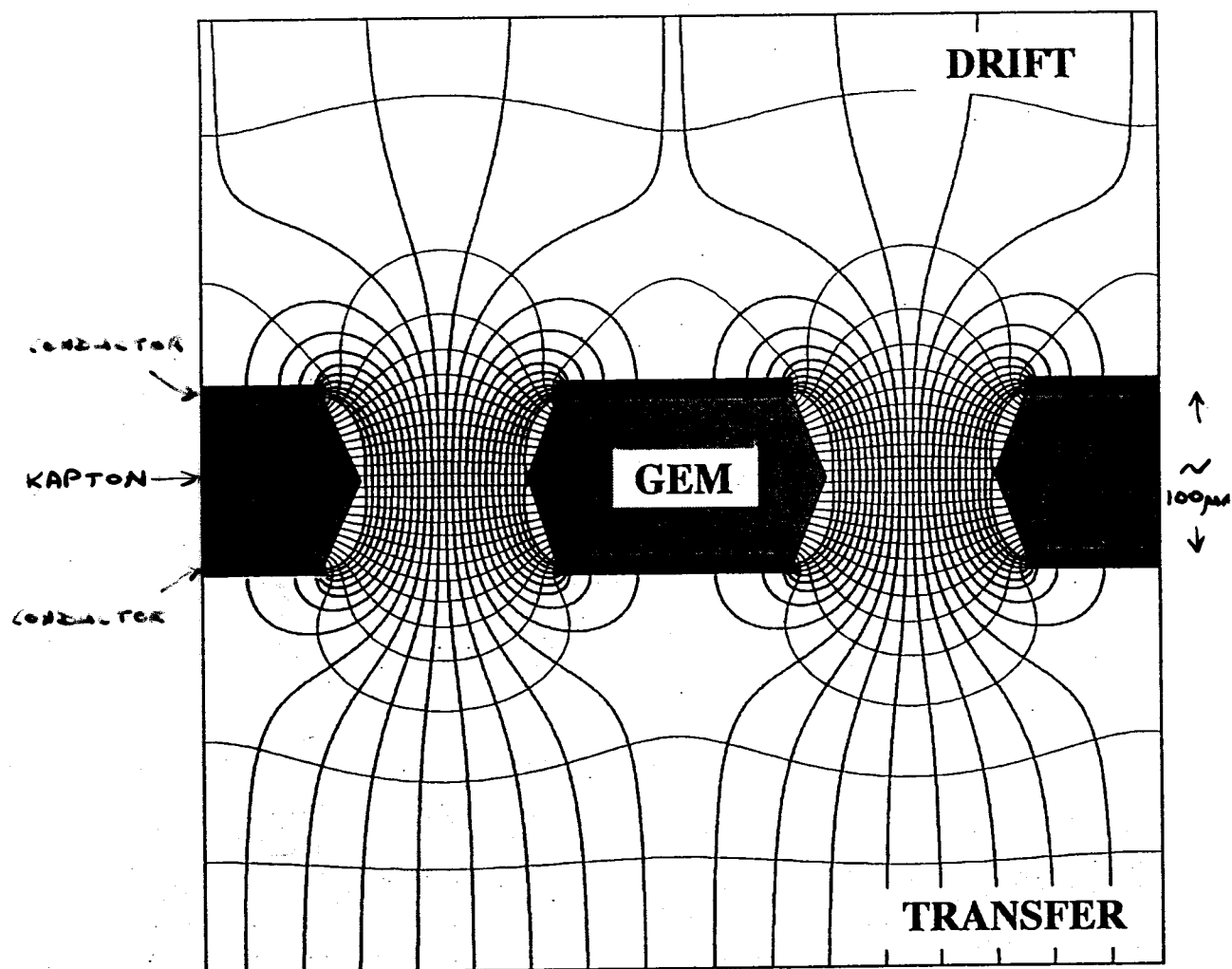


Figure 34 Electric field and equipotential lines in the gas electron multiplier.

with the transfer field; the balance is collected by the lower GEM electrode (183). The large increase of charge at the highest fields corresponds to the onset of charge multiplication in the transfer gap. The current caused by positive ions is divided between the top GEM and the drift electrodes; its constancy demonstrates that the true gain is unaffected by the value of the transfer field. Similar measurements provide the effect of the drift field in the collection efficiency, or transparency.

Single and double GEM detectors with PCB readout have been extensively tested in the laboratory and in particle beams (184). Figure 39 shows the large efficiency plateau and the position resolution as a function of voltage obtained with a double GEM device.

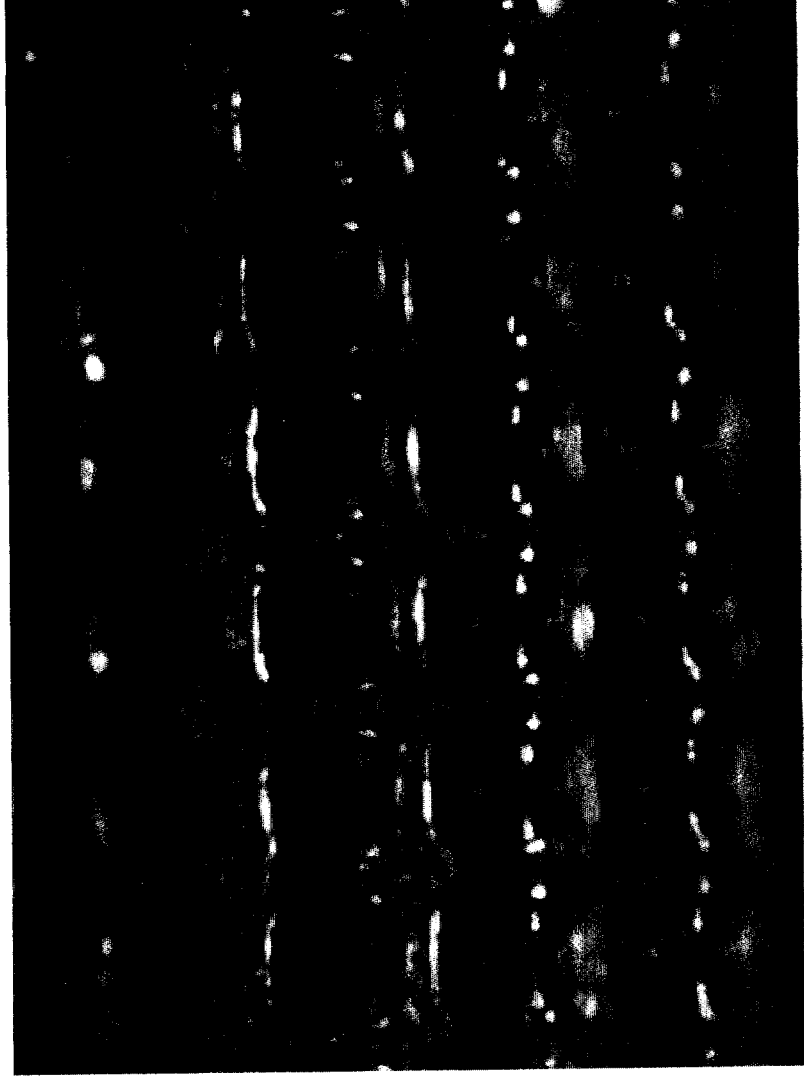
In this mode of operation, the signal detected on the strips is entirely due to the electrons collection, without a slow ion tail, and is typically a few tens of nanoseconds wide for a 1-mm-wide gap. The method can be extended to obtain a projective two-dimensional readout, using double-level thin polymer foil with pads or strips interconnected in various patterns (see Figure 40) as pick-up electrodes (185). Both readout electrodes are kept at ground potential, giving the double GEM a

Gas Electron Multiplier (GEM)

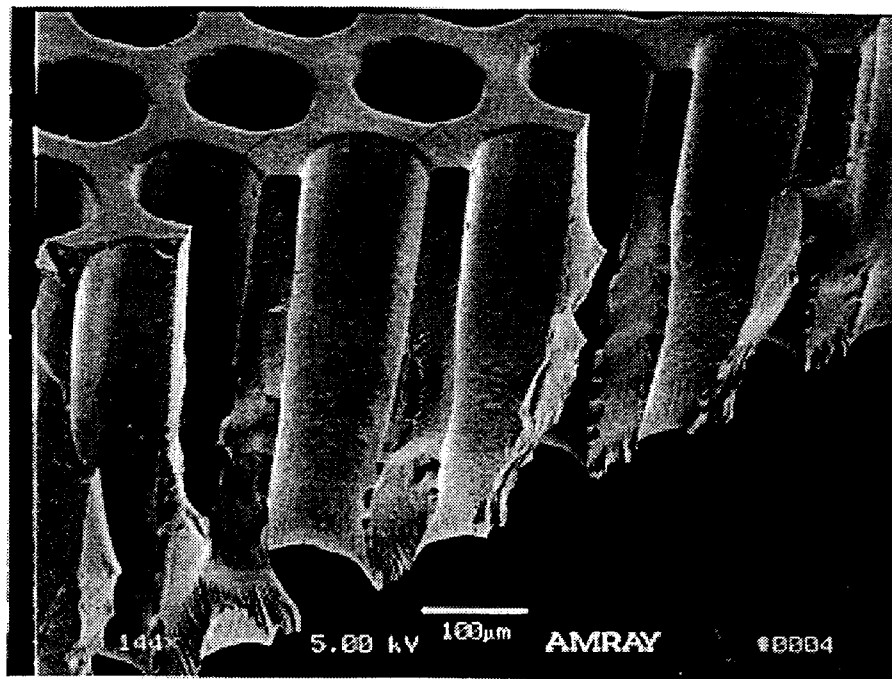
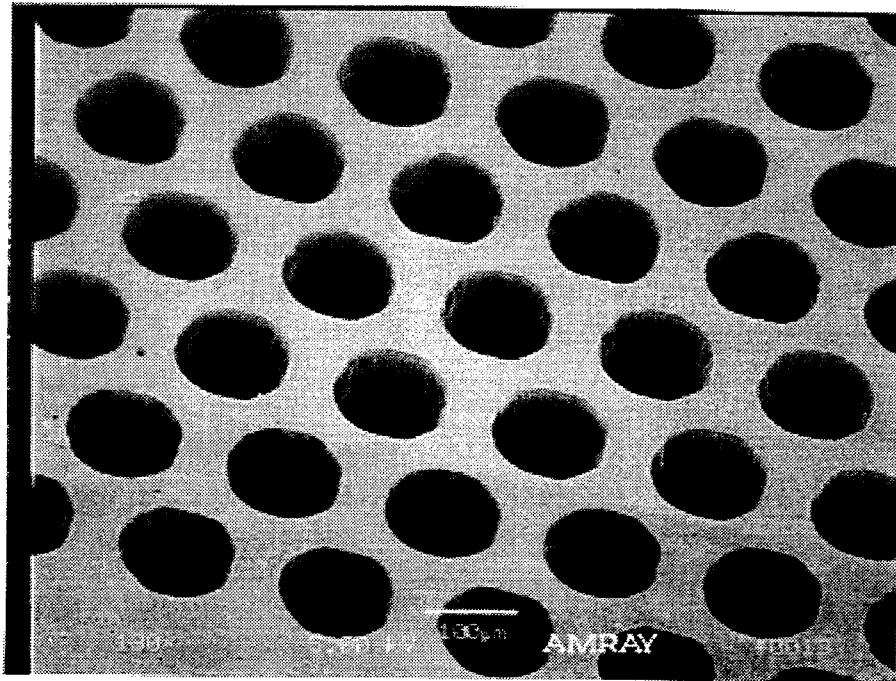
Fabio Sauli, NIM A 386 (1997) 531-534

GEM manufactured by
chemical etching of Kapton

100 μm



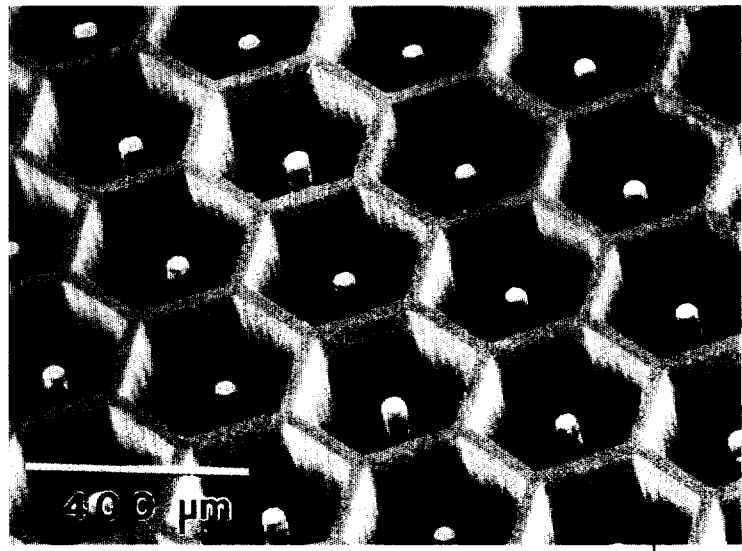
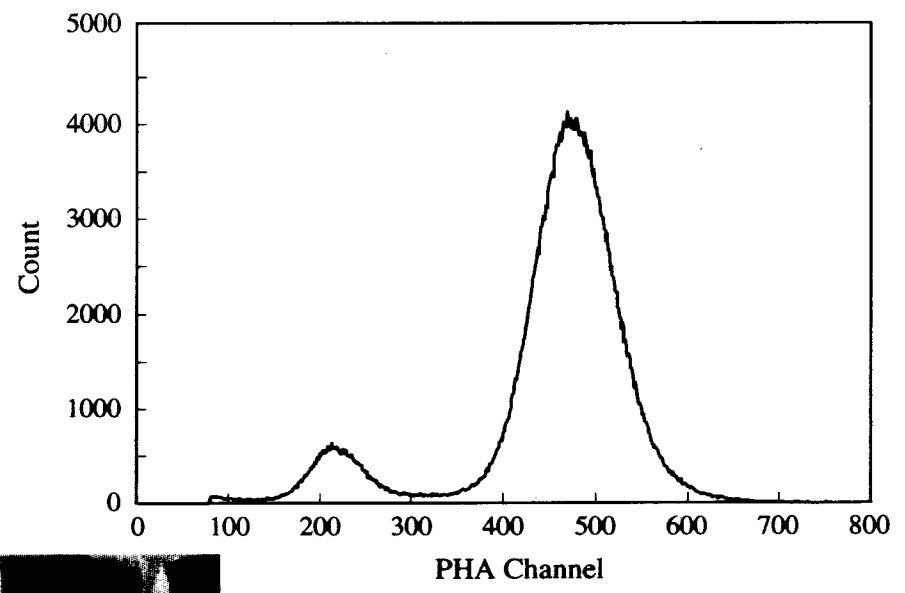
GEM / SU8 – Electron Microscope Photographs (2)



Preliminary Results from the Pin Array (MIPA)

Anode Pulse Height Spectrum

Collimated 5.4keV x-rays



Gas Gain vs. Anode Bias

